Polymer Journal, Vol. 24, No. 11, pp 1251—1258 (1992)

Crystal Structure of the ω-Helical Form of Poly[β-(p-methylbenzyl) L-aspartate]

Shintaro SASAKI and Shigeo KIMURA

Department of Polymer Chemistry, Tokyo Institute of Technology, Ookayama, Meguro-ku, Tokyo 152, Japan

(Received April 8, 1992)

ABSTRACT: The monoclinic crystal structure of the left-handed ω-helical form of poly[β-(p-methylbenzyl) L-aspartate] was analyzed by X-ray diffraction method. The main chain assumes the 4_3 helix, but the side-chain arrangement around the axis is deformed from the fourfold symmetry. The structure is statistically disordered in the manner of both arrangements of up and down helices and interpenetration of the methylbenzyl groups. The side-chain conformation is extended essentially with *trans* about χ_1 and *gauche* about χ_2. The distance $b(O_1^{\delta 1}, N_5)=0.32$ nm and the infrared absorption suggests a certain interaction between the main-chain amino group and the side-chain carbonyl group.

KEY WORDS Poly[β-(p-methylbenzyl) L-aspartate] / X-Ray Diffraction / ω-Helix / Crystal Structure / Helix Sense / Side Chain Conformation /

Conformational versatility of polyaspartates has been extensively studied with respect to the helix sense and the ω-helix formation.[1-5] Poly(β-benzyl L-aspartate) (PBLA) exists as the left-handed α-helix (α_L) in the chloroform solution.[2,3] On heating the film above 160°C, the molecular conformation is irreversibly transformed from the α_L into the left-handed fourfold helix (ω_L) having unit height $p=0.1325$ nm.[5] Its crystal structure is compatibly tetragonal. In contrast, poly[β-(p-chlorobenzyl) L-aspartate] (Cl-PBLA) takes on the right-handed α-helix (α_R) in the solution.[2,3] Its film exhibited a transition at about 190°C from the α_R into the ω-helix with $p=0.130$ nm.[6] This ω-helix had been misunderstood as right-handed,[6,7] but the sense was confirmed to be left-handed by the conformational energy calculation[8] and the circular dichroic measurement.[9]

Helix-sense inversion associated with the solid-state transition was also observed for poly[β-(p-methylbenzyl) L-aspartate] (Me-PBLA).[9] The ω_L forms of Cl-PBLA and Me-PBLA are monoclinic (not tetragonal), *i.e.*, the side chains do not conform to the fourfold screw symmetry even if the main chain assumes the 4_3 helix. From similar intensity distribution and isometrical unit cells, their crystal structures are expected to be isomorphous. In this paper, we report the crystal structure of the highly-crystalline ω_L form of Me-PBLA.

EXPERIMENTAL

The samples of Me-PBLA were prepared by polymerization of the *N*-carboxy anhydride in 1,2-dichloroethane using triethylamine as the initiator. They were recovered by precipitation with methanol, and identified by the NMR spectrum. The density of the film was measured at 25°C by the flotation method using the mixed solvent of carbon tetrachloride and cyclohexane.

X-Ray diffraction photographs were taken with Ni-filtered Cu-K_α radiation. Oriented films were prepared by stroking the liquid-

crystalline concentrated solution in chloroform onto a glass plate. Reflection spacings were calibrated against the 111 reflection of silicon powder sprinkled over the specimen. Intensities were measured by scanning the photographs with a microphotometer and corrected for the Lorentz-polarization factors.

RESULTS AND DISCUSSION

The film of Me-PBLA exhibited two irreversible transitions on heating by differential scanning calorimetry; one was exothermic at 140°C and the other was endothermic at 210°C. These were identified to be associated with the α_R-to-ω_L transition, and the transition from the ω_L to the β pleated-sheet structure, respectively.[9]

The diffraction pattern of the as-cast film was explained by the standard α_R structure.[1,6] Figure 1a shows the characteristic pattern of oriented film annealed at 120°C. The crystallinity was improved by heat treatment. The meridional reflection corresponding to the α-helical unit height was observed at 0.150 nm, and the intense fifth layer line supported the standard helix pitch of 0.54 nm. The crystal structure was hexagonal with the lateral dimension $a=1.49$ nm (exactly equal to that of Cl-PBLA[6]). The calculated density 1.26 g cm^{-3} agreed with the observed value.

The diffraction pattern of the film annealed at 150°C is shown in Figure 1b. From the circular dichroism, the helix sense was certified to be left-handed.[9] The unit height was determined to be 0.132 nm from the meridional reflections with spacings of 0.264 and 0.132 nm. The spacings of 21 equatorial and eleven first-layer-line reflections were elucidated by the monoclinic unit cell with $a=1.66$ nm, $b=1.34$ nm, c(fiber axis)$=0.528$ nm, and $\gamma=108°$ (Table III). Since $c/p=4$, the main chain assumes the ω-helical conformation. One chain passes through the unit cell, and the calculated density 1.30 g cm^{-3} is consistent with the observed value 1.28 g cm^{-3}. The possible space group is $P2_1$-C_2^2.

In the crystal of the α_R form of Cl-PBLA, the up-pointing (U) and down-pointing (D) helices were arranged at random.[6] For the ω_L form of Cl-PBLA, a tetragonal unit cell with $a=2.33$ nm containing one U chain and one D chain was once proposed.[6] This suggested that a large amount of molecular movement occurred at the α_R-to-ω_L transition to make up the systematic arrangement of U and D helices. However, this tetragonal unit cell is impossible, as is evident merely by considering the crystal density.[9] The true unit cell is monoclinic containing one (U or D) chain. We consider that large-scale molecular movements causing positional exchange of U and D helices take place hardly by heat treatment.[10] Accordingly, a disordered distribution of U and D helices may occur similarly for the α_R and the ω_L forms of Me-PBLA.

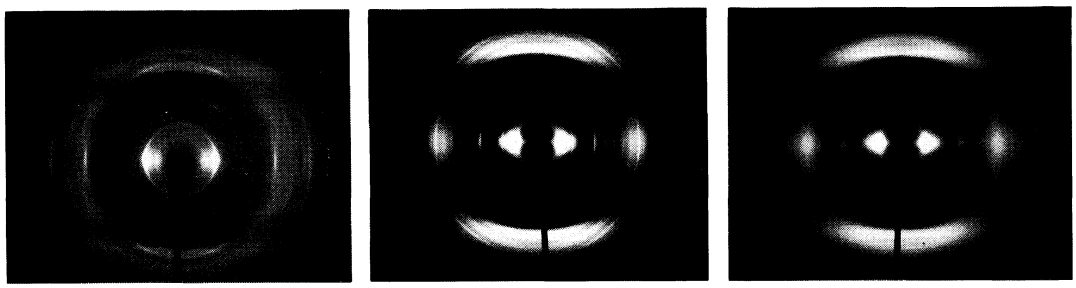

Figure 1. X-Ray diffraction patterns of the α_R form (a), ω_L form (b), and non-crystalline ω form (c) of Me-PBLA. The orientation direction is vertical.

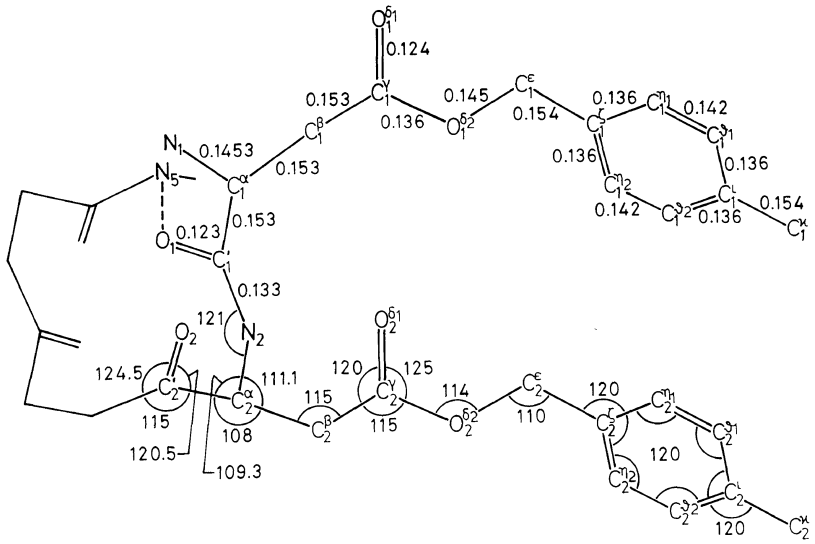

Figure 2. Designation of atoms, bond lengths (upper, in nm) and bond angles (lower, in deg).

In addition to the crystalline ω_L form, the non-crystalline ω form (Figure 1c) was occasionally obtained. The preparation condition was not clear. As judged from the unit height $p=0.130$—0.132 nm, the molecular structure is of the ω-helical, but the arrangement is positionally disordered.

In order to cope with the limited diffraction data of the crystalline ω_L form, structure analysis was performed by employing the linked-atom least-squares method (LALS),[11-13] in which the bond lengths and the bond angles were kept to their standard values given in Figure 2.[7] Analysis was initially carried out in the c projection using only equatorial data. Missing reflections were included in the LALS refinement, assuming zero intensity. The structure factors were calculated by neglecting the hydrogen atoms and assuming appropriate temperature factors (Table II).

The main-chain model was built up for the rigid 4_3 helix, since the diffraction data were insufficient to refine the delicate distortion from the 4_3 helix. As described in the preceding paper,[9] the conformational energy was minimized with the torsion angles using empirical energy functions. The set of $\phi=71.5°$, $\psi=46.9°$, and $\omega=174.5°$, giving the hydrogen-bond distance $b(O_1, N_5)=0.283$ nm, was considered to be most reasonable. The side-chain models were explored with combinations of *trans* (T) and *gauche* (G and $\bar{G}$) forms for χ_1, χ_2, and χ_4. The torsion angle χ_3 about the ester bond was fixed at 180°. The torsion angle χ_5 about the rotation of the phenylene group was assumed to be 90° by referring to conformational statistics on crystal structures of globular proteins.[14]

The "monoclinic" crystal system claims, at least for the side-chain arrangement, deviation from the original ω-helical symmetry. In the first place, however, analysis was undertaken by placing the 4_3 molecular models at the origin of the unit cell. Molecular rotation about the c axis was restricted so that the bulky methylbenzyl (MBz) groups should not be located around the special positions (x, y)=(0, 1/2), (1/2, 0), and (1/2, 1/2). If the MBz groups were at these places, regular interpenetration might occur between adjacent helices. Such a stacking is impossible for the helix with the short repeat distance $c=$ 0.528 nm. Structure factor calculations were repeated by placing U and D helices in various

orientations, but any reasonable structure to explain the observed equatorial intensities could not be found. The molecular models with the twofold screw axis were also examined, in which the side chains were allowed to take two distinctive conformations alternately. However, all our trials were unsuccessful.

Another approach was then attempted in order to estimate the locations of the MBz groups. Since the two-dimensional structure in the c projection is centrosymmetric, the structure factors of the $hk0$ reflections are real. Therefore, the electron-density projection can be calculated by assigning the phase factors ($+1$ or -1) to the amplitudes ($|F_o|$'s) obtained from the intensity data:

$$\rho(xy)=\frac{1}{c}\int_0^c \rho(xyz)\mathrm{d}z$$
$$=\frac{1}{V}\sum_h\sum_k F_o(hk0)\cos\{2\pi(hx+ky)\} \quad (1)$$

where V is the unit-cell volume. Because one chain passes through the unit cell, the crystal structure factors coincide with molecular structure factors. In the case of cylindrical molecules, the structure factors are contributed mainly by zero-order Bessel function, and the sign is positive for lower diffraction angles while negative for higher angles. The crossover, depending upon the radial size of the helix, takes at R_o (reciprocal spacing)$=$ 1.5—2 nm^{-1} for the models of Me-PBLA.

The Fourier projection was calculated by assuming (a) $F_o>0$ for $R<R_o$ and $F_o<0$ for $R>R_o$, and (b) equal $|F_o|$ values for the overlapped reflections. Amplitudes were corrected to those on the absolute scale by referring to the results of trial calculations. Since the ω-helical structure is not cylindrical, the above assumptions do not entirely hold. Therefore, the map may be false partly, but it contains some valid indications. The pattern of the map was not affected seriously by R_o. Figure 3a shows the map when $R_o=1.8\,\mathrm{nm}^{-1}$, in which the helix core is seen clearly. Some side chains seem to extend in a direction perpendicular to the b axis. Furthermore, density concentrations appear near special positions (1/2, 0) and (0, 1/2). When a side chain occupies the particular special position and the fifth residue is stacked just above the first residue, the nearby side chain of the adjacent helix must avoid that position; *i.e.*, two different conformations (with one half probability for each) must be defined for equivalent (the first and the third) residues. Accordingly, the molecular chain has the 2_1 symmetry only in a statistical manner,

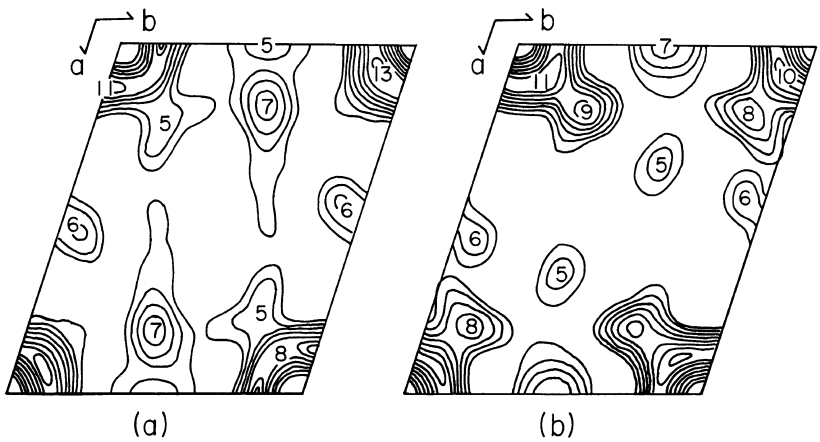

Figure 3. Equatorial electron-density projection of Me-PBLA. The figures indicate the density in units of 100 electron nm^{-3} (a) A test pattern (see the text). (b) The final map.

where distinctive side-chain conformations are sequent irregularly.

By taking into account the features of the electron-density map, structure models were sought for two categories of models (I) (χ_1, χ_2)=(T, G) and (II) ($\bar{G}$, T). Model (I) includes the $Lt(-)$ conformation proposed by Scheraga *et al.*[4a] The extended side-chain conformation can be built up by introducing the T form for χ_4, while the bent conformation to occupy the special position (0, 1/2) is produced by the G or skew (S) form for χ_4. For a reasonable arrangement of the side chains, the superposed D helix was produced by 180° rotation of the U helix about the a^* axis. As a result of LALS refinements, model (I) was found to explain the observed intensities; the discrepancy factor between the observed and calculated intensities, $R_d = \sum|\sqrt{I_{obs}} - \sqrt{I_{calc}}|/\sum\sqrt{I_{obs}}$, was 0.18 for all reflection data including the missing reflections. Twelve parameters were adjusted here; the molecular translation along the c axis, the rotation about the axis, nine side-chain torsion angles, and the scale factor. Model (II) could explain the equatorial data, but the R_d factor increased to 0.31 when the first-layer-line data were included.

The side-chain torsion angles were not uniquely defined; they converged to slightly different values depending on the initial values. Standard deviations were in the range of 5—12°. The most probable values are listed

Table I. Side-chain conformations and torsion angles (deg)[a]

	χ_1	χ_2	χ_3	χ_4	Weight
Side chain 1	*T*	*G*	*T*	*T*	1
(Extended)	161	33	180	215	
Side chain 2-1	*T*	*G*	*T*	*T*	0.5
(Extended)	180	69	180	195	
2-2	*T*	*G*	*T*	*S*	0.5
(Bent)	167	41	180	131	

[a] Angle χ_3 and χ_5 were fixed at 180° and 90°, respectively.

Table II. Orthogonal atomic coordinates[a] and temperature factors of the ω_L from of Me-PBLA

Atom	*X*/nm	*Y*/nm	*Z*/nm	*B*/nm²
Main chain 1				
N_1	0.059	0.162	−0.191	0.05
C_1^{α}	0.178	0.177	−0.110	0.05
C_1'	0.185	0.062	−0.009	0.05
O_1	0.209	0.084	0.110	0.05
C_1^{β}	0.176	0.308	−0.032	0.05
Main chain 2				
N_2	0.162	−0.059	−0.059	0.05
C_2^{α}	0.177	−0.178	0.022	0.05
C_2'	0.062	−0.185	0.123	0.05
O_2	0.084	−0.209	0.242	0.05
C_2^{β}	0.308	−0.176	0.100	0.05
Side chain 1				
C_1^{γ}	0.271	0.314	0.088	0.07
$O_1^{\delta 1}$	0.240	0.380	0.188	0.10
$O_1^{\delta 2}$	0.386	0.244	0.073	0.10
C_1^{ε}	0.475	0.251	0.188	0.15
C_1^{ζ}	0.621	0.252	0.142	0.20
$C_1^{\eta 1}$	0.684	0.370	0.115	0.25
$C_1^{\eta 2}$	0.689	0.134	0.126	0.25
$C_1^{\theta 1}$	0.819	0.370	0.073	0.25
$C_1^{\theta 2}$	0.823	0.135	0.083	0.25
C_1^{ι}	0.886	0.253	0.057	0.20
C_1^{κ}	1.033	0.254	0.011	0.25
Side chain 2-1				
C_2^{γ}	0.333	−0.298	0.189	0.07
$O_2^{\delta 1}$	0.331	−0.286	0.313	0.10
$O_2^{\delta 2}$	0.356	−0.414	0.122	0.10
C_2^{ε}	0.379	−0.528	0.208	0.15
C_2^{ζ}	0.439	−0.644	0.127	0.20
$C_2^{\eta 1}$	0.574	−0.656	0.115	0.25
$C_2^{\eta 2}$	0.357	−0.735	0.068	0.25
$C_2^{\theta 1}$	0.629	−0.763	0.039	0.25
$C_2^{\theta 2}$	0.412	−0.842	−0.007	0.25
C_2^{ι}	0.547	−0.854	−0.020	0.20
C_2^{κ}	0.607	−0.970	−0.101	0.25
Side chain 2-2				
C_2^{γ}	0.320	−0.280	0.211	0.07
$O_2^{\delta 1}$	0.370	−0.250	0.320	0.10
$O_2^{\delta 2}$	0.271	−0.403	0.180	0.10
C_2^{ε}	0.282	−0.501	0.287	0.15
C_2^{ζ}	0.148	−0.572	0.307	0.20
$C_2^{\eta 1}$	0.120	−0.686	0.238	0.25
$C_2^{\eta 2}$	0.057	−0.522	0.395	0.25
$C_2^{\theta 1}$	−0.004	−0.752	0.258	0.25
$C_2^{\theta 2}$	−0.067	−0.588	0.414	0.25
C_2^{ι}	−0.095	−0.702	0.345	0.20
C_2^{κ}	−0.230	−0.774	0.366	0.25

[a] X, Y, and Z axes are directed to a^*, b, and c axes, respectively.

Table III. Observed and calculated d spacings and intensities of the ω_L from of Me-PBLA

Indices	d_{calc}/nm	d_{obs}/nm	$\sqrt{I_{obs}}$	$\sqrt{I_{calc}}$
1 0 0	1.58	1.57	80	74
0 1 0	1.28	1.28	42	40
−1 1 0	1.19	1.18	34	27
1 1 0	0.871	0.87	28	33
−2 1 0	0.790	0.79	44	38
2 0 0	0.789			
−1 2 0	0.669	0.67	38	47
0 2 0	0.640	0.639	26	17
−2 2 0	0.595	0.595	44	34
2 1 0	0.595			
−3 1 0	0.550	0.55	33	37
1 2 0	0.538			
3 0 0	0.526	0.529	49	58
−3 2 0	0.487	0.488	49	42
−1 3 0	0.448	0.448	82	82
3 1 0	0.441			
−2 3 0	0.436	0.43	51	53
2 2 0	0.436			
0 3 0	0.426			
−4 1 0	0.415			
−3 3 0	0.397	0.396	38	30
−4 2 0	0.395			
4 0 0	0.395			
1 3 0	0.383	—	—	2
3 2 0	0.356	0.35	24	31
−4 3 0	0.348			
4 1 0	0.348			
−2 4 0	0.335	0.334	55	46
−1 4 0	0.334			
2 3 0	0.334			
−5 1 0	0.331			
−5 2 0	0.326	0.32	48	38
−3 4 0	0.321			
0 4 0	0.320			
5 0 0	0.316	—	—	0
−5 3 0	0.302	0.30	46	50
−4 4 0	0.298			
4 2 0	0.297			
1 4 0	0.296			
3 3 0	0.290	0.29	25	28
5 1 0	0.287			
−6 2 0	0.275	0.275	27	32
−6 1 0	0.275			
−5 4 0	0.270	0.270	41	32
−2 5 0	0.269			
2 4 0	0.269			
1 0 1	0.501	0.49	55	58
0 1 1	0.488			
−1 1 1	0.483			
1 1 1	0.452	0.452	51	58
−2 1 1	0.439	0.438	46	41
2 0 1	0.439			

Table III. (Continued)

Indices	d_{calc}/nm	d_{obs}/nm	$\sqrt{I_{obs}}$	$\sqrt{I_{calc}}$
−1 2 1	0.415	0.41	55	56
0 2 1	0.407			
−2 2 1	0.395	0.395	42	51
2 1 1	0.395			
−3 1 1	0.381	0.378	35	29
1 2 1	0.377			
3 0 1	0.373			
−3 2 1	0.358	0.358	21	12
−1 3 1	0.342	0.338	50	41
3 1 1	0.339			
−2 3 1	0.336			
2 2 1	0.336			
0 3 1	0.332	—	—	15
−3 3 1	0.317	0.316	25	35
−4 2 1	0.316			
4 0 1	0.316			
1 3 1	0.310	—	—	15
3 2 1	0.295	0.295	25	29
−4 3 1	0.291			
4 1 1	0.291			
−2 4 1	0.283	0.282	29	25
2 3 1	0.282			
−1 4 1	0.283			
−5 1 1	0.281			

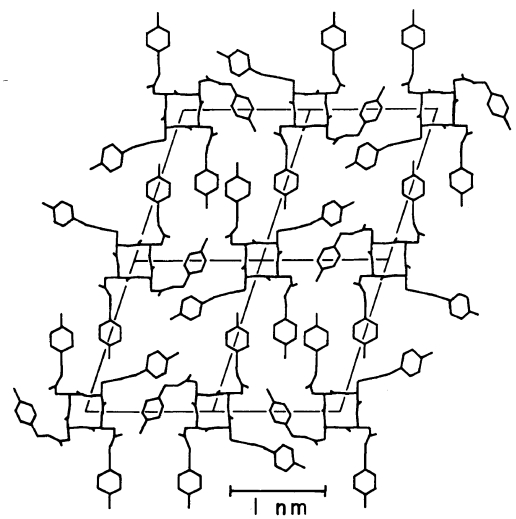

Figure 4. A model of two-dimensional packing that is probable where the U and D helices are arranged alternately.

in Table I. The side chain of residue 1 is extended, while that of residue 2 is assumed to be either extended or slightly bent. The latter corresponds to the $Lt(-)$ conformation. The atomic coordinates of the successive two residues of the U helix (pointing the C-terminal end to the $+Z$ direction) are listed in Table II. They are given in the orthogonal coordinates in nm. The X, Y, and Z axes are directed to the a^*, b, and c axes, respectively (Figure 4). The coordinates of the D helix are obtained by transformations $(X, -Y, -Z)$ from the given coordinates. The observed and calculated intensities are compared in Table III. Figure 3b shows the electron-density map calculated by assigning the final phase factors to the observed equatorial intensities, where for the overlapped reflections the amplitudes were distributed proportionally to the calculated ones .

It is certain that the molecular structure is not regular regarding side-chain conformation. It may seem strange, however, to assume that the side chain of the first residue is extended while that of the second residue is either extended or bent with equal probability (Table I). Structure models in which the side chain of the first residue took on two conformations were also examined, but the R_d factor could not be improved. There was no evidence to support the more complicated structure. Although some ambiguities are inevitable, it is fair to offer a simple structure if it gives the minimum R_d factor.

The structure proposed here is considered possible, since the MBz groups pack reasonably. A packing model, probable in the area in which the U and D helices are arranged alternately, is illustrated in Figure 4. Depending upon the manner of chain arrangement, various packing patterns can be built. The molecular backbone is roughly the 4_3 helix, but distorted irregularly. The packing pattern must be understood as different along the c axis. This means that the MBz groups interpenetrate between adjacent helices irregularly.

Table IV. Infrared characteristic absorption of Me-PBLA

Form	Band position/cm^{-1}		
	Amide A	Amide I	Ester ν(C=O)
α_R	3280	1659	1741
ω_L	3300	1672	1730

Although the fiber repeat distance is too short to accept the regular stacking of MBz groups of neighboring helices, the statistical molecular deformation enables interpenetration, which may contribute to stabilization of the ω_L structure.

Infrared spectral changes associated with the α_R-to-ω_L transition also support the side-chain conformation with T about χ_1 and G about χ_2. The main-chain hydrogen bond is formed between the C=O group of the first residue and NH group of the fifth residue. The distance was set to be $b(O_1, N_5)=$ 0.283 nm. In the analyzed structure, the N_5H group is associated also with the carbonyl oxygen atom of the side chain of the first residue, the distance being $b(O_1{}^{\delta 1}, N_5)=$ 0.32 nm. This contact is close enough to suggest bifurcated hydrogen bonds. Even if it is judged not to be bifurcated, an appreciable interaction is expected. In the previous paper,[9] it was shown that infrared characteristic bands of amide A and amide I shifted to the higher frequencies by the α_R-to-ω_L transition (Table IV); *i.e.*, the main-chain hydrogen bond is rather weak in the ω_L helix. The stretching vibration of the side-chain carbonyl group shifted to the lower frequency, suggesting that a certain interaction is built up for the side-chain carbonyl group. These spectral features are consistent with the side-chain conformation analyzed by X-ray diffraction.

REFERENCES

1. R. D. B. Fraser and T. P. MacRae, "Conformation

in Fibrous Proteins," Academic, New York, N.Y., 1973.
2. (a) M. Hashimoto and A. Aritomi, *Bull. Chem. Soc. Jpn.*, **39**, 2707 (1966). (b) M. Hashimoto and S. Arakawa, *Bull. Chem. Soc. Jpn.*, **40**, 1698 (1967).
3. (a) R. H. Karlson, K. S. Norland, G. D. Fasman, and E. R. Blout, *J. Am. Chem. Soc.*, **82**, 2268 (1960). (b) E. M. Bradbury, B. G. Carpenter, and R. M. Stephens, *Biopolymers*, **6**, 905 (1968); *Macromolecules*, **5**, 8 (1972).
4. (a) J. F. Yan, G. Vanderkooi, and H. A. Scheraga, *J. Chem. Phys.*, **49**, 2713 (1968). (b) J. F. Yan, F. A. Momany, and H. A. Scheraga, *J. Am. Chem. Soc.*, **92**, 1109 (1970). (c) R. F. McGuire, G. Vanderkooi, F. A. Momany, R. T. Ingwall, G. M. Crippen, N. Lotan, R. W. Tuttle, K. L. Kashuba, and H. A. Scheraga, *Macromolecules*, **4**, 112 (1971).
5. (a) E. M. Bradbury, L. Brown, A. R. Downie, A. Elliott, R. D. B. Fraser, and W. E. Hanby, *J. Mol. Biol.*, **5**, 230 (1962). (b) J. P. Baldwin, E. M. Bradbury, I. F. McLuckie, and R. M. Stephens, *Macromolecules*, **6**, 83 (1973).
6. Y. Takeda, Y. Iitaka, and M. Tsuboi, *J. Mol. Biol.*, **51**, 101 (1970).
7. Y.-C. Fu, R. F. McGuire, and H. A. Scheraga, *Macromolecules*, **7**, 468 (1974).
8. Y. Takeda, *Biopolymers*, **14**, 891 (1975).
9. S. Sasaki, H. Ogawa, and S. Kimura, *Polym. J.*, **23**, 1325 (1991).
10. S. Sasaki and M. Dairaku, *Macromolecules*, **23**, 4939 (1990).
11. (a) S. Arnott and A. J. Wonacott, *Polymer*, **7**, 157 (1966); *J. Mol. Biol.*, **21**, 371 (1966). (b) S. Arnott and E. Selsing, *J. Mol. Biol.*, **88**, 509 (1974).
12. (a) Y. Takahashi, T. Sato, H. Tadokoro, and Y. Tanaka, *J. Polym. Sci., Polym. Phys. Ed.*, **11**, 233 (1973). (b) Y. Takahashi and H. Tadokoro, *Macromolecules*, **6**, 672 (1973).
13. (a) S. Sasaki, Y. Takahashi, and H. Tadokoro, *J. Polym. Sci., Polym. Phys. Ed.*, **10**, 2363 (1972). (b) S. Sasaki and Y. Iwanami, *Macromolecules*, **21**, 3389 (1988). (c) S. Sasaki, T. Yamamoto, T. Kanbara, A. Morita, and T. Yamamoto, *J. Polym. Sci., B, Polym. Phys.*, **30**, 293 (1992).
14. T. N. Bhat, V. Sasisekharan, and M. Vijayan, *Int. J. Peptide Protein Res.*, **13**, 170 (1979).